Sensors & Transducers, Vol. 196, Issue 1, January 2016, pp. 24-29

Sensors & Transducers

http://www.sensorsportal.com

Coherent Anti-Stokes and Coherent Stokes in Raman Scattering by Superconducting Nanowire Single-Photon Detector for Temperature Measurement

[1] Annepu Venkata Naga Vamsi and [2] Annepu Bhujanga Rao
[1] Dept. of Electronics and Instrumentation Engineering, Gitam University, Visakhapatnam, India
[2] Dept. of Instrument Technology, Andhra University, Visakhapatnam, India
[1] Tel.: +91-9550417485
E-mail: vamsi9441105975@gmail.com

Received: 20 November 2015 /Accepted: 30 December 2015 /Published: 31 January 2016

Abstract: We have reported the measurement of temperature by using coherent anti-Stroke and coherent Stroke Raman scattering using superconducting nano wire single-photon detector. The measured temperatures by both methods (Coherent Anti-Raman scattering & Coherent Stroke Raman scattering and TC 340) are in good accuracy of ± 5 K temperature range. The length of the pipe line under test can be increased by increasing the power of the pump laser. This methodology can be widely used to measure temperatures at instantaneous positions in test pipe line or the entire temperature of the pipe line under test. *Copyright © 2016 IFSA Publishing, S. L.*

Keywords: Coherent anti-Stroke Raman scattering, Coherent Rayleigh-Brillouin scattering, Superconducting nanowire single photon detector, Quantum mechanics, Cryostat.

1. Introduction

In the process of light scattering, the most critical factor is the length scale of any or all of these structural features relative to the wavelength of the light being scattered. In all the light-scattering processes treated so far, Pan X., *et al.* has reported the utilization of the coherent Rayleigh scattering (CRS) to measure the temperature of the low density gases and weakly ionized plasma [1]. Later Graul J., *et al.* has reported the measurement of the temperature in the molecular gas by utilizing the coherent Rayleigh-Brillouin scattering method [2]. Gu Z. has reported the spectrometer for the measurement of spontaneous Rayleigh-Brillouin (RB) scattering line profiles at ultraviolet wavelengths from gas phase molecules [3]. In the recent work by Yu Zhang., *et al.* has reported the coherent anti-Strokes Raman scattering with single molecule sensitivity using a plasmonic Fano resonance [4]. Zumbush A., *et al.* has reported three-dimensional vibrational imaging by coherent anti-Stroke Raman scattering [5]. Mathew P. Thariayn, *et al.* has reported the dual pump coherent anti-Strokes Raman scattering system for temperature and species measurement in an optically accessible high pressure gas turbine combustor facility [6]. Russel Lockett, *et al.* has come up with the similar ay of temperature measurement in an internal combustion engine by coherent anti-Stroke Raman spectroscopy [7].

This has motivated to work on the coherent stroke and coherent anti-Stroke Raman scattering for measurement of the temperature by utilizing the superconducting nanowire single photon detector in a single mode fiber.

In this paper we have worked on the single mode fibers by considering the incident radiation as one monochromatic wave of frequency ω_1. We now consider the experimental situation illustrated in Fig. 1 where the incident radiation consists of two overlapping coherent monochromatic beams of frequencies ω_1 and ω_2, with $\omega_1 > \omega_2$. As the overlapping beams of radiation propagate through the material system, new radiation is produced with frequencies corresponding to various combinations of ω_1 and ω_2. From amongst the possible combinations we first consider the combination $2\omega_1 - \omega_2$. If we vary ω_2 while keeping ω_1 constant we find that the intensity of the scattering increases dramatically when $\omega_1-\omega_2=\omega_M$, where ω_M is a molecular frequency that can be observed in Raman scattering. When this frequency-matching condition is satisfied $\omega_s=\omega_1+\omega_M$, because $\omega_s=2\omega_1-\omega_2=\omega_1+(\omega_1-\omega_2)=\omega_1+\omega_M$.

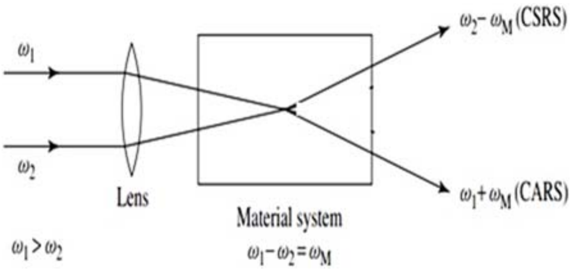

Fig. 1. Diagrammatic representations of CARS (coherent anti-Stroke Raman scattering), CSRS (coherent stroke Raman scattering).

The condition $\omega_1 - \omega_2 = \omega_M$ can be regarded as a Raman resonance. This is quite different from the electronic resonances described earlier. The scattered frequency $\omega_1 + \omega_M$ has the form of an anti-Stokes Raman frequency relative to ω_1. As this scattered radiation is coherent, it is called Coherent anti-Stokes Raman Scattering, or CARS. By varying ω_2 over a range of values that covers the desired values of ω_M a CARS spectrum can be obtained. The CARS frequencies will be superimposed on a background of weak non-resonant scattering given by $2\omega_1 - \omega_2$. If alternatively we consider the scattered frequency combination $2\omega_2 - \omega_1$, then when $\omega_1 - \omega_2 = \omega_M$ strong scattering now occurs at $\omega_2 + (\omega_2 - \omega_1) = \omega_2 - \omega_M$. This is Stokes radiation relative to ω_2 and is called Coherent Stokes Raman Scattering or CSRS.

CARS and CSRS differ in many important respects from the Raman processes. They produce highly directional beams of scattered radiation with small divergences. The scattered intensity is proportional (a) to the square of the number of scattering molecules and (b) to the square of the irradiance of the incident radiation at ω_1 and to the irradiance of the incident radiation at ω_2. Consideration of the interaction of the waves of frequencies ω_1 and ω_2 involves the bulk or macroscopic properties of the material system which must then be related to the individual or microscopic properties of the molecules. From such considerations emerge the special properties of CARS and CSRS radiation which we have just outlined energy change in the material system and the process is said to be passive or parametric. The material system acts as a facilitating agent as it were for the exchange of energy between radiation of different frequencies and this is very effective when $\omega_1 - \omega_2 = \omega_M$. Energy level diagrams for CARS and CSRS and given in Fig. 2 (a) and (b) respectively.

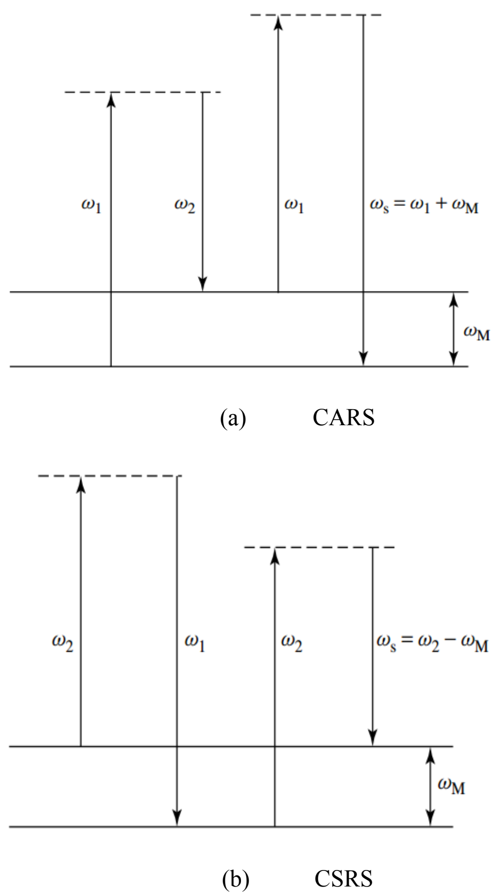

Fig. 2. (a) Energy level diagrams for CARS, b) Energy level diagrams for CSRS.

2. Methodology

2.1. Quantum Mechanics (QM) Domain

In the Quantum Mechanics (QM) domain, a harmonic oscillator oscillates at an angular frequency ω_M with quantized energy levels:

$$E_n = (n+1)\,\hbar\,\omega_M,\ n = 0, 1, 2, 3 \ldots \qquad (1)$$

According to the statistical mechanics if such a quantum oscillator is in contact with a thermal reservoir of temperature T then this oscillator has probability P_n being in the energy level E_n given by:

$$P_n = \exp\left(-\frac{\left(n+\frac{1}{2}\right)\hbar\omega M}{K_B T}\right) / \sum_{\acute{n}=0}^{\infty} \exp\left(-\frac{\left(\acute{n}+\frac{1}{2}\right)\hbar\omega M}{K_B T}\right) \qquad (2)$$

Here K_B is the Boltzmann constant, and ħ= h/2π with h to be the Planck constant. Furthermore according to the QM the dipole transition strength from energy level $E_n \rightarrow E_{n+1}$ is found proportional to quantum number n in the following:

$$|p|_{n,n+1} \propto \sqrt{n+1} \quad (3)$$

Now we can evaluate the Stokes line strength from an ensemble of *N* identical oscillators connected to a thermal bath at temperature *T*

$$N\sum_{n=0}^{\infty}(\sqrt{n+1})^2\ P_n = \frac{N}{1-\exp(-\frac{\hbar\,\omega M}{K_B T})} \quad (4)$$

Conversely, the dipole transition strength from energy level $E_{n+1} \rightarrow E_n$ is found in the following proportion

$$|p|_{n+1,n} \propto \sqrt{n} \quad (5)$$

For the anti-Stokes line strength of an ensemble of *N* identical oscillators:

$$N\sum_{n=0}^{\infty}(\sqrt{n})^2\ P_n = \frac{N}{\exp\left(-\frac{\hbar\,\omega M}{K_B T}\right)-1} \quad (6)$$

We could write down the strength of the Raman Stokes line λ_s from an ensemble of identical QM oscillator ω_M that is dominated by the induced electric dipole radiation:

$$I_S = I_o(\frac{\ell}{\lambda_s})^4\ \frac{1}{1-\exp(-\frac{\hbar\,\omega M}{K_B T})} \quad (7)$$

Here ℓ is a length scale and I_O an intensity scale proportional to the incident light strength. At the same time the associated anti-Stokes Raman line λ_{AS} has the strength:

$$I_{AS} = I_o\,(\frac{\ell}{\lambda_{AS}})^4\ \frac{1}{\exp\left(\frac{\hbar\,\omega M}{K_B T}\right)-1} \quad (8)$$

We thus derived the expression that can be served as the basis for the Raman temperature sensor:

$$\frac{I_{AS}}{I\ _S} = (\frac{\lambda_s}{\lambda_{AS}})^4\ \exp\left(-\frac{\hbar\,\omega M}{K_B T}\right) \quad (9)$$

The above formula is derived with the assumption that each molecule is independent in the system and their mutual interactions are only represented by a statistical temperature parameter *T*. So by theoretical approach we have come to a conclusion that the coherent anti-Stokes and coherent stroke Raman scatterings, we can calculate the temperature inside a closed or open pipelines accurately. Hence by the above technique we report the measurement of the temperature experimentally by the Superconducting nanowire single – photon detector (SNSPD).

3. Experimental Setup

The light source is a fiber laser with a repetition frequency of 36 MHz and centered near 1550 nm. The sensing fiber is a standard low-loss single-mode fiber with a diameter of 10.1 µm and attenuation less than 0.2 dB/km at a wavelength of 1550 nm. We used filter for flittering the pump laser to a 1 nm line width at a wavelength of 1530.47 nm. We used a variable attenuator before amplifying the pump laser with an erbium doped amplifier (EDFA). The attenuator is used to minimize pulse distortion due to gain saturation in the amplifier. We used a pulse picking modulator applied to our pump laser for extending the test fiber in lengths on the order of kilometers.

The pump signal is again filtered post-amplification to remove the broad band from the pump, which could otherwise be backscattered in the fiber under test and create unwanted pulse counts at the SNSPD detectors, as the filters used before and after the amplifier can only provide 20-30 dB rejection of unwanted wavelengths. We thus injected the pump laser light into the fiber under test(FUT) via a fiber coupling (fiber-optic circulator).we have tested the fiber up to a length of 5 meters as it is limited by the repetition rate of our pump laser. This test fiber is passed through a pipeline of 5 meters in length for the experimentation work. This pipe is wrapped with electrical wire at 3 meter position for creating a localized hot spot externally by applying the current to the electrical wire for the temperature measurement inside the pipeline with respect to the wavelengths and the coherent stroke counts and coherent anti-Stroke counts. The backscattered light from the fiber under test is directed by the circulator to a series of filters that will reject the pump wavelength. Without these filters, we would have unwanted photons of the pump wavelength reaching the SNSPD detector. The 1350 nm filters are used to block any of the EDFA photons that might reach the SNSPD detectors.

Now the process of band splitters to separate and filter the Raman backscattered photons into an S-band channel (1450 nm-1490 nm) and an L-band channel (1550 nm – 1630 nm). The light from the S-band and L-band channels are coupled to SNSPDs, where accurate and precise temperature measurement and control is one of the key factors for this experiment.

We used Temperature Controller 340 (MAKE: Lakeshore) a device that measures and displays temperatures. We have installed the TC 340 at the position where the external electrical wire is wrapped around the pipe line, so as to compare the temperature at the 3 meter position by the proposed method and as well as to measure the temperature at the 3 meter position by the temperature controller (TC 340) to strengthen the results of our experimented method.

In the cryostat, the voltage passes through the low-pass filter that is part of the printed circuit board, and reaches the contact pads. The pulse signal is picked up from the sample holder with a coaxial cable, passes into a signal inverting cryogenic amplifier with a bandwidth of 30 MHz to 2.1 GHz and is brought outside the cryostat. From there, a semi rigid coaxial cable passes the signal through a −3 dB attenuator to a second amplifier. The −3 dB attenuator damps reflections between the amplifiers and prevents the formation of a standing wave. After the second amplifier the signal is damped by −6 dB before it reaches the oscilloscope. Before the signal cable enters the oscilloscope or the pulse counter.

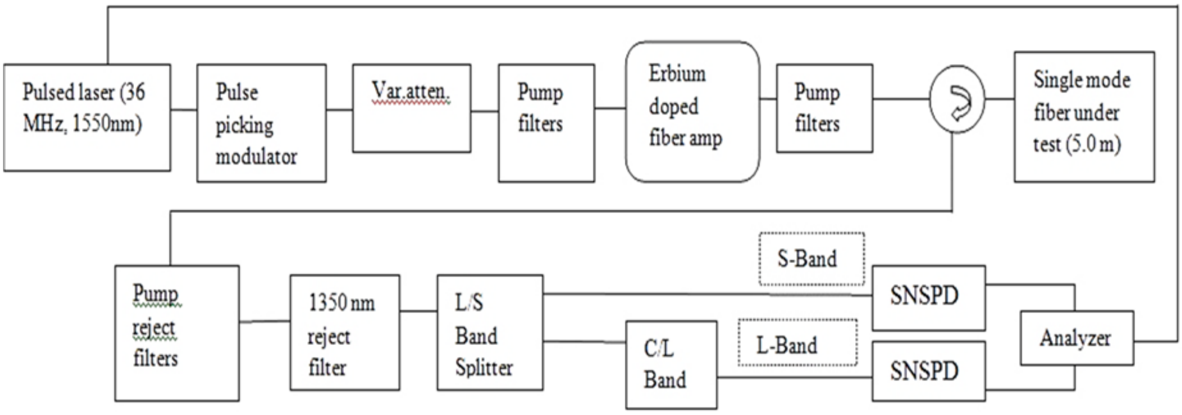

Fig. 3. Measurement set up for wavelengths analysis's of coherent anti-Stoke Raman Scattering and coherent stroke Raman Scattering in the fiber under test.

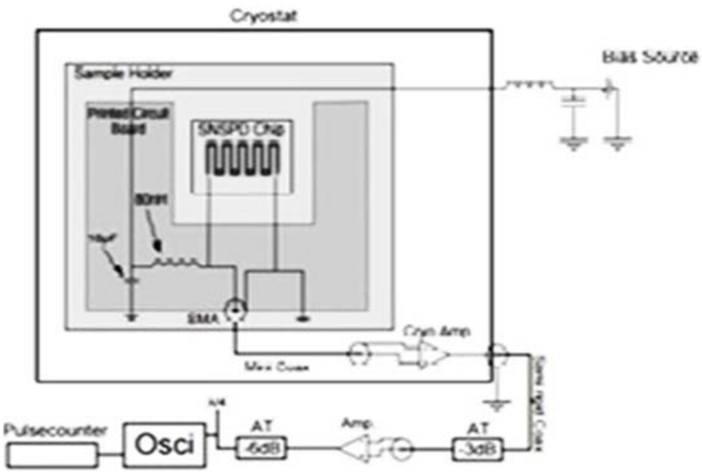

Fig. 4. Sketch of the electronic setup. The printed circuit board is mounted on the sample holder right next to the SNSPD chip with the amplification and bias.

4. Results and Discussion

We modeled the Raman backscattering by the strokes and anti-Strokes as follows:

$$\text{Backscattered photons } (I_u) \approx \eta_u \, \Delta V_u \, P_0 \, L|g_R| N D_c, \tag{10}$$

where I_u is the backscattered photons per second, η_u is the detection efficiency (DE) of the SNSPDs, ΔV_u is the bandwidth of the stroke and anti-Stroke filters, P_0 is the peak pump power, L is the fiber length, g_R is the Raman gain factor, D_c is the duty cycle of the pump signal, N represents the photon population as given in the Equations (4) and (6) respectively.

By the theory of quantum Mechanics, the Raman gain generally increases, on the order of 0.8 W^{-1}. k m^{-1} . As our pump power is limited by gain saturation in our EDFA to around P_{ave} = 18 mW. This configuration achieved count rates of approximately 3×10^5 Hz at room temperature. Thus with the ratio of strokes to anti-Strokes as given by Equation (9) and the instantaneous position in the fiber under test (FUT) is given by

$$\frac{I_{AS}(x)}{I_S(x)} = \left(\frac{\lambda_S}{\lambda_{AS}}\right)^4 \exp\left(-\frac{\hbar\,\omega \mathrm{M}}{K_B T(x)}\right), \tag{11}$$

where I_S is the strokes count, I_{AS} is the anti-Strokes count, x is the position in the FUT, and $(\frac{\lambda_S}{\lambda_{AS}})^4$ which include the detection efficiency of the two SNSPDs detectors.

So by the Equation (11) we have calculated the temperature of the entire fiber under test as a function of desired position. We have calculated the input intensity and output intensity with respect to the power. The normalized intensity vs. the power (mW) is shown in the Fig. 5 where the input intensity is represented by a blue line and the output intensity is represented by red color line.

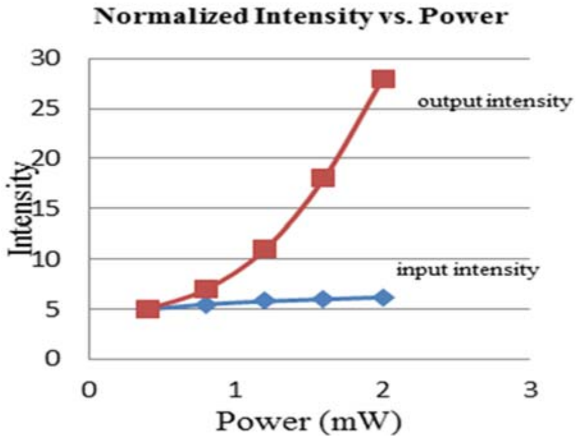

Fig. 5. The normalized Intensity vs. Power.

Now by having the output intensity, the coherent anti-Stroke counts for the different wavelengths of the strokes and anti-Strokes. We have the coherent anti-Stroke counts vs. the wavelength as show in the Fig. 6.

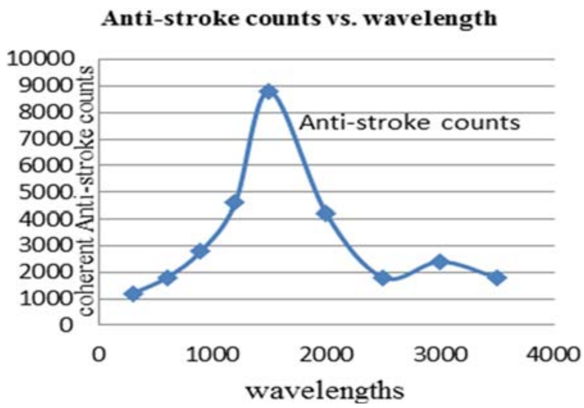

Fig. 6. Coherent anti-Stroke counts vs. wavelength.

Thus as we already wrapped the electrical wire around the test pipe at 3 meters, which will create a localized hot spot in the test fiber and by this we were able to have the temporal profile of the single mode fiber under test at the desired position and the temperature spike at the 3 meters position is plotted and is as shown in the Fig. 7.

We have obtained the temperature at the 3 m position by the TC 340 and the measured temperature is 455 K and the measured temperature by proposed method is 450 K. The proposed methodology has a very good accuracy of ± 5 K. So by using the CARS and CSRS we were able to measure the temperature at a fixed position or we can also measure the entire temperature profile of a tunnel or a lengthily pipe line.

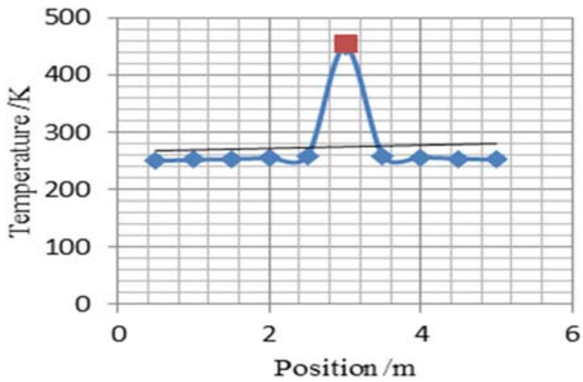

Fig. 7. The result of the temperature measurement from TC 340 (Red colour spike at 3 m position) and the temperature measurement by the proposed method (Blue colour spike at 3 m position).

5. Conclusions

In this paper, we have experimented and demonstrated that the coherent stroke and coherent anti-Stroke Raman Scattering can be used for measurement of the temperature profile by using superconducting nano wire single – photon detector. We have tested the pipe line of 5 meters length by externally giving temperature at 3 meter distance and achieved the temperature profile at that position as shown in the Fig. 7 we have achieved the same temperature by TC 340 which strengthens the temperature measurement by CARS and CSRS using SNSPDs. We can increase the length of the test pipe by increasing the power of the pump laser. This methodology is therefore particularly suitable for applications to large or elongated structures; such as dams, large bridges and pipelines.

References

[1]. Pan X., Barker P. F., Meschanov A., Grinstead J. H., Shneider M. N., Miles R. B., Temperature measurement by coherent Rayleigh scattering, *Optics Letters*, Vol. 27, No. 3, 1 Feb. 2002, pp. 161-163.

[2]. Graul J., Lilly T., Coherent Rayleigh-brillouin scattering measurement of atmospheric and molecular gas temperature, *Optics Express*, Vol. 22, Issue 17, 2014, pp. 20117-20129.

[3]. Gu Z., Vieitez M. O., Van Duijn E. J., Ubachs W., A Rayleigh-brillouin scattering spectrometer for ultraviolet wavelengths, *Rev. Sci. Instrum.*, Vol. 83, No. 5, May 2012, 053112.

[4]. Yu Zhang, Yu-Rong Zhen, Oara Neumann, Jared K. Day, Coherent anti-Stokes Raman scattering with single-molecule sensitivity using a plasmonic Fano resonance, *Nature Communications*, Vol. 5, June 2014, pp. 1-7.

[5]. Zumbusch A., Holtom G. R., Xie X. S., Three-dimensional vibrational imaging by coherent anti-Stokes Raman scattering, *Phys. Rev. Lett.*, Vol. 82, No. 20, Aug. 1999, pp. 4142-4145.

[6]. M. P. Thariayn, Dual-pump coherent anti-Stokes Raman scattering system for temperature and species measurement in an optically accessible high pressure gas turbine combustor, *Measurement Science and Technology*, Vol. 22, No. 1, 2010.

[7]. Russel Lockett, Coherent anti-Stokes Raman spectroscopy temperature measurements in an internal combustion engine, *Optical Engineering*, Vol. 33, No. 9, 1994, pp. 2870-2874.